International Journal of Mechanical, Industrial and Aerospace Sciences
ISSN: 2517-9950
Vol:5, No:2, 2011

Energy Systems and Crushing Behavior of Fiber Reinforced Composite Materials

Hakim S. Sultan Aljibori

Abstract**—**Effect of geometry on crushing behavior, energy absorption and failure mode of woven roving jute fiber/epoxy laminated composite tubes were experimentally studied. Investigations were carried out on three different geometrical types of composite tubes (circular, square and radial corrugated) subjected to axial compressive loading. It was observed in axial crushing study that the load bearing capability is significantly influenced by corrugation geometry. The influence of geometries of specimens was supported by the plotted load – displacement curves of the tests.

Keywords**—**Crushing behavior, jute fiber, composite tubes and Specific energy absorption

I. Introduction

THE awareness of environmental sustainability drives the automotive industry to utilize natural fibers. Since natural fibers are a readily available resource with a relatively low price, therefore, natural fibers play an important role in seeking renewable materials for automotive utilizations [1].

Raw materials from natural to man-made fibers are eligible to be used in matrix composites. However, natural fibers, such as flax, hemp, jute and cotton, show an advantageous property for composite reinforcement because they have lower density than glass and carbon fibers, thus yielding a relatively lighter weight composite. For instance, Joshi (2004) highlighted that natural fiber components can significantly reduce the weight of a composite material. Joshi further supported with the example of replacement of conventionally produced side panel by Acrylonitrile Butadiene Styrene (ABS) material. The automotive side panel weighs 2480 lbs. (1,125 kg) with ABS material. In contrast, natural fiber composite material, such as hemp-Epoxy can offer a weight reduction of 27% [2]. Some of the other advantages of natural fibers are cost efficiency, availability, and nontoxic in nature [3]. Dweib stated that the availability of natural fibers is considered to be advantageous because "it reduces dependency on foreign and domestic petroleum oil". Flax and other fibers, such as hemp, jute, ramie and kenaf are the most commonly used in composite application because of their properties. The most important of their properties as it relates to composite is their excellent tensile strength, high durability and low density [4]. As seen in Table 1 and Table 2, flax fibers have the highest Young's modulus and tensile strength compared to other natural fibers. Even though the tensile strength of flax fibers is not as high as E-glass fibers, the density of flax fibers is relatively low compared to E-glass, which makes flax fibers lighter. In contrast, for car seat frames, steel has a density of 7.85 g/cm^3, which is more than five times higher than that of flax at 1.4 g/cm^3 [5]. Table 2 presents comparison of mechanical properties of flax with other high performance fibers.

TABLE I
COMPARISON OF YOUNG'S MODULUS OF SEVERAL BAST AND SYNTHETIC FIBER COMPOSITES [6]

Fiber Type	Young's modulus (Gpa)
Flax	100
Hemp	69
Jute	64
Ramie	59
Rayon carbon fiber	34-55
Glass fiber	70-85
Aramid fiber, Kevlar	60-200
Silicon carbide	190
Polyacrylonitrile carbon fiber	230-490

TABLE II
PROPERTIES OF GLASS AND NATURAL FIBERS [6]

Properties	Fiber Type				
	Flax	Hemp	Jute	Ramie	E-glass
Density (g/cm^3)	1.4	1.48	1.46	1.5	2.55
Tensile Strength (N/m^2)	800 – 1500	500 – 900	400 – 800	500	2400
Elastic modulus (GPa)	60 – 80	70	10 – 30	44	73
Specific modulus (GPa)	26 – 46	47	7 – 21	29	29
Elongation at failure (%)	1.2 – 1.6	1.6	1.8	2	3
Moisture Absorption (%)	7	8	12	12 - 17	-

Santulli C. [7] studied jute/polyester woven laminates having thickness of 3 and 5 mm were tested in a Rosand IFW5 drop-weight impact tower with impact energies up to 20 Joules and at impact velocity of 2 m/s. The diameter of the hemispherical impactor was 12.7 mm. During dart penetration tests, the jute fibre reinforced laminates appeared slightly

Hakim S. Sultan Aljibori [1*], Faculty of Computing, Engineering & Technology, Asia Pacific University College of Technology and Innovation (UCTI), Technology Park Malaysia, Bukit Jalil, 57000 Kuala Lumpur Malaysia (e-mail: dr.hakim@ucti.edu.my).

Dhafer A. Shnawah[2], Department of Mechanical Engineering, University of Malaya, 50603 Kuala Lumpur, Malaysia.

curved at energies not exceeding 30% of the measured penetration energy (Around 125 kJ/m²), pointing the presence of internal damage although they were not appeared at the surface (Figure1). Some other evidence of damage was identified by the thermoelastic stress measurements, where delamination was found to be characteristically concentrated on a line along the external boundary of the area under impact force (Figure 2). This suggests that resin-rich areas and more in general, the presence of manufacturing defects have an influence on impact damage propagation. In terms of penetration energy, the values obtained for jute fibre composites were in the range of about one third of those obtained for glass fibre composites with the same amount of fibre content. However, in the case of Charpy impact tests, the difference is much larger (around 30 kJ/m² compared to around 200 kJ/m² for glass fibre composites). This was explained by the fact that the material does not undergo penetration until a wide amount of matrix cracking takes place and drives the fibre to be torn off [8], which refers a higher impact damage tolerance and good capacity of sustaining load after damage initiation. However, the impact damage characterization on jute fibre reinforced laminates [9] reveal that their interlaminar adhesion is sufficient to yield a conical through-the-thickness impact damage pattern which is typical in stronger composites and often referred to as reversed-pine tree (Fig.3).

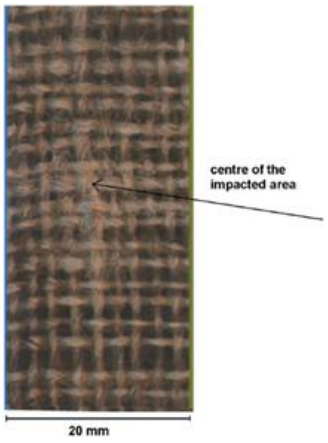

Fig. 1 Impact damage of jute/polyester composites

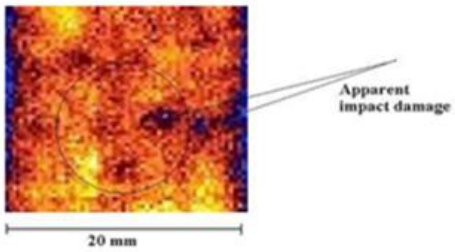

Fig. 2 Thermoplastic stress analysis of impacted jute/polyester composites

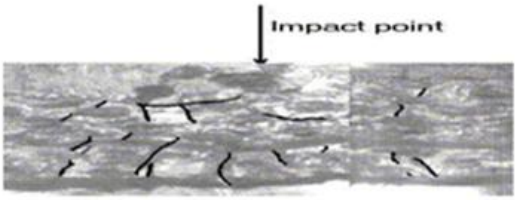

Fig. 3 Conical pattern of impact damage in jute-polyester composites

II. Experimental Setup

A. Geometry and Materials

Three types of specimen have been investigated, SJFT, CJFT and RCJFT. The entire structures are made of woven roving jute fiber/epoxy as shown in Figure 4. Three specimens were fabricated under the same conditions with a fixed fiber orientation angle of 0°/90° and epoxy resin (ZE-LAM 7892 A) with hardener (ZE-LAM 7892 B). All the specimens have inside diameter (d) 10 cm, height (h) 10 cm and wall thinness (t) 5mm. Three types of wooden mandrels have been manufactured in the workshop. The mandrels have the same length of 30 cm as shown in Fig 5.

Fig. 4 Jute Fiber, Epoxy with hardener

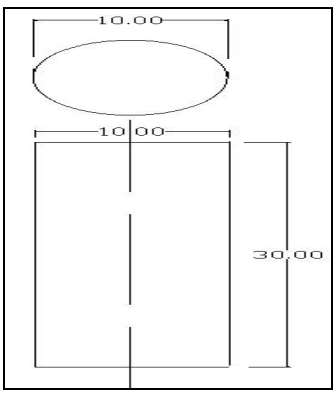

Fig. 5 (a) SJFT

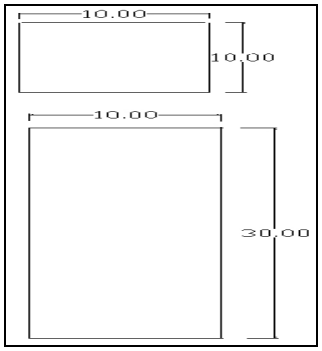

Fig 5. (b) CJFT

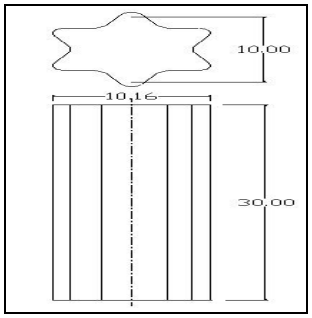

Fig 5. **(c)** RCJFT

Fig. 5 Schematic shows the top and front view of specimens

B. Fabrication process

The principle of wet hand lay-up process was used for the fabrication. The tube was fabricated by rolling the woven roving jute fiber on the rotating wooden mandrel. The woven roving jute fiber was passed through a resin bath by using a brush to make sure the specimens have equal amount of epoxy/resin, causing resin impregnation. The fabricated tube was cured 24 hr at room temperature (26ºC) to provide optimum hardness. Then the cured tube was extracted from the mandrel and it became ready for cutting into the desired damnations by using cutting machine. Specially designed mandrel was used for fabrication of specimen. The mandrel is divided into two halves for easy assemble after curing. Epoxy/resin was used as a matrix of the composite structure. 100 ml of resin was mixed carefully with 20 ml of hardener and an electrical mixture machine was used to produce an excellent mixture. The fabrication process of composites was carried out under the same condition for the three different geometrical shapes of the composites with the fixed fiber orientation of ±0°/90°.

C. Tensile Test

The mechanical properties of jute fabric/epoxy composite materials have been investigated by using the INSTRON tensile testing machine, where the specimen is subjected to tension as shown in Figure 6. Mechanical properties of jute fiber/epoxy composite material are listed in Table 3.

Fig. 6 Set Up of Tensile Test

TABLE III
MECHANICAL PROPERTIES OF JUTE FABRIC COMPOSITE

Displacement at Max. Load(mm)	2.6
Max. Load (KN)	3.15
Stress at Max. Load (MPa)	56.86
Strain at Max. Load (%)	5.2
Ultimate Stress(Mpa)	2.6
Modulus (AutYoung) (Mpa)	1526.786
Energy at Breaking Point (J)	3.847

D. Testing procedure

The specimens were tested in quasi-static axial compression between two flat steel plates one is static and the other one moving with constant crushing speed. INSTRON 4469 digital testing machine (Figure. 7) with full scale load range of 50kN was used. Three specimens of each type of composite tubes were tested. Load platens were set parallel to each other before testing. All composite tubes were compressed at a loading rate of 15 mm/min until limited crush, which implies complete compaction of the tubes being tested. Load and displacement were recorded by an automatic data acquisition system. Progress and history of triangular crushing test of SJFT, CJFT and RCJFT are shown in Figures 8-10.

Fig. 7 Photograph of the INSTRON machine

Fig. 8 Progress of Crashing Test of SQJFT

Fig. 9 Progress of Crashing Test of CJFT

Fig.10 Progress of Crashing Test of RCJFT

III. Results And Discussion

A. Load Displacement Curve

The mode of failure and the pattern of load–displacement curves of the various composite tubes are different, so each one has been discussed independently for axial load in the following sections:

- *SJFT*

The load-displacement curve is divided into two regions as shown in Figure 11, the first region started from 0kN and raised through the elastic zone until it reached a value of load 34.85kN at 2.82 mm displacement as presented in Figure 11b. After this point, the curve passed the elastic zone and started crushing through the plastic zone, the curve dropped dramatically as shown in Figure 8c, and that was attributed to an extensive longitudinal unstable brittle fracture occurred at the corners of the structure. The non-progressive crushing of the SJFT tube is initiated with crack formation and fracture at the corners of the square tube due to local stress concentration, at the end of the linear elastic loading phase, when the applied load attains a peak value of F_i. The crack formation at the tube corners is followed by an immediate drop of the compressive load, and its propagation parallel to the tube axis results in splitting of the square tube into four parts. Furthermore, subject to the compressive load, each of these parts is splitted into irregular shapes of the tube; this kind of failure causes catastrophic and the absorbed crash energy is very small compared to the stable progressive end crushing mode failure.

- *CJFT*

Figure 12 (a) shows a typical crushing deformation of the CJFT subjected to quasi-static compressive load. Non-linearity is evident during the pre-crush-stage as shown in Figure 9b, where non-axisymmetric buckling is seen, which is characterized by unstable local tube wall buckling initiated the failure at the top end of the specimen as shown in Figure 12b. In this stage the tube resistance reaches its first and highest peak (45.35kN) at a deformation of 4.44 mm. On the other hand, the tube load-carrying capacity decreases gradually with the progress of crushing process. It is seen that the progressive folding in buckling is characterized by hinge formation and folding of the tube walls as in the case of ductile fiber-reinforced materials with the development of wrinkles. These wrinkles and buckles initiate and develop sequentially from one end of a tube under buckling process. The accumulation of the materials of the specimen caused the growth in the load/displacement curve at the end as shown in Figure 12c.

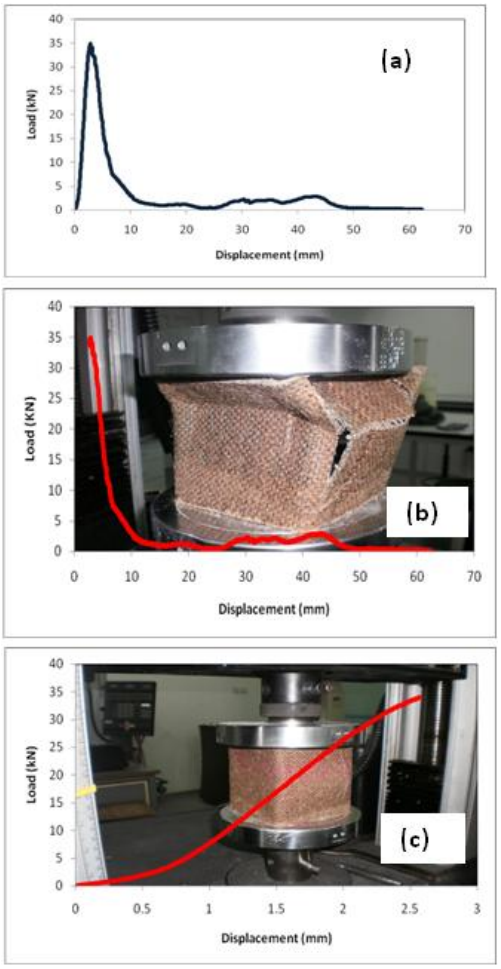

Fig. 11 Load-Displacement Curve of SJFT

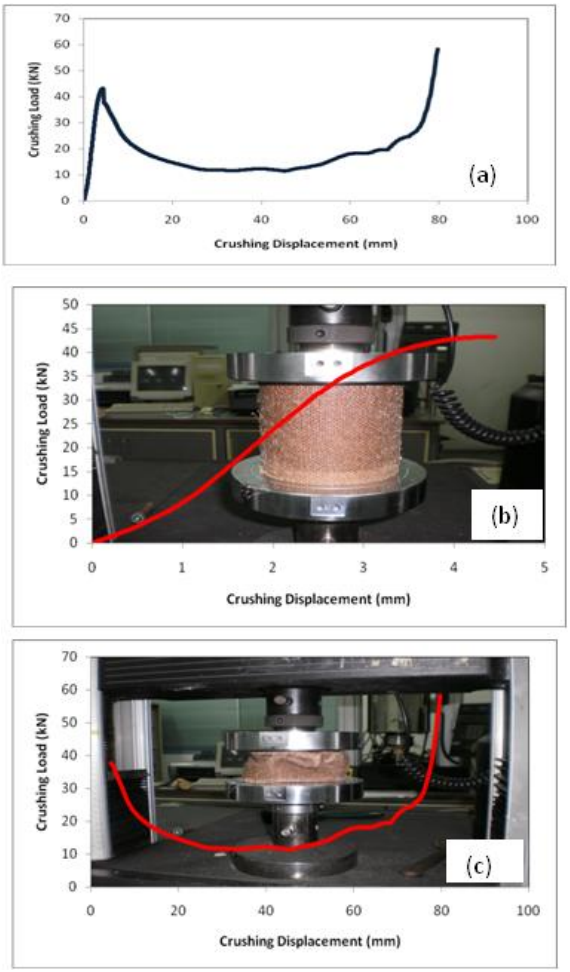

Fig. 12 Load-Displacement Curve of CJFT

- *RCJFT*

Figure 13 shows a crushing deformation of the RCJFT, subjected to quasi-static compressive load, which is characterized by longitudinal fracture, crack propagation and splitting of the tube walls transversely to the tube longitudinal axis. This is typically initiated at the top end of the compressed tube associated with low crash energy absorption compared to the stable progressive end-crushing mode. In this mode, the audible matrix cracking and fiber breakage occurred when the tube wall resistance reaches its peak magnitude of 38.84 KN at 5.77 mm as shown in Figure 130-a and13-b. It is observed that the tube resistance sharply reduces with the progress of crushing and the tube walls were splitting transversely with rapid propagation of brittle fracture in the corrugated walls of the tube leading to a catastrophic failure as shown in Figure 13c.

Figure 14 represent the load-displacement curves of three different geometries for comparison between three shapes. Crushing loads of the specimens listed are in Table 4.

B. Crashworthiness Parameters

The energy absorbing capability can be estimated by knowing different parameters. These parameters are illustrated in Table 5 and explained in the following sections.

- *Initial Failure Load (Fi)*

Initial failure load or the first peak crush failure load, is the boundary between the pre-crushing zone (elastic) and the post-crushing zone (plastic). Before arriving at this point, the structure has the ability to return back to the original state. After the initial failure load, the structure deforms permanently. It is useful to find the range of the temporary deformation region and the permanent deformation region of the structures. Figure 15 shows the variation of the initial crushing load due to the change of the geometry of the tubes. The circular tubes (CJFT) yield the highest initial crushing load of 45.35 kN. The corrugated tubes (RCJFT) followed the CJFT and produced initial crushing load higher than those of the square tubes (SJFT).

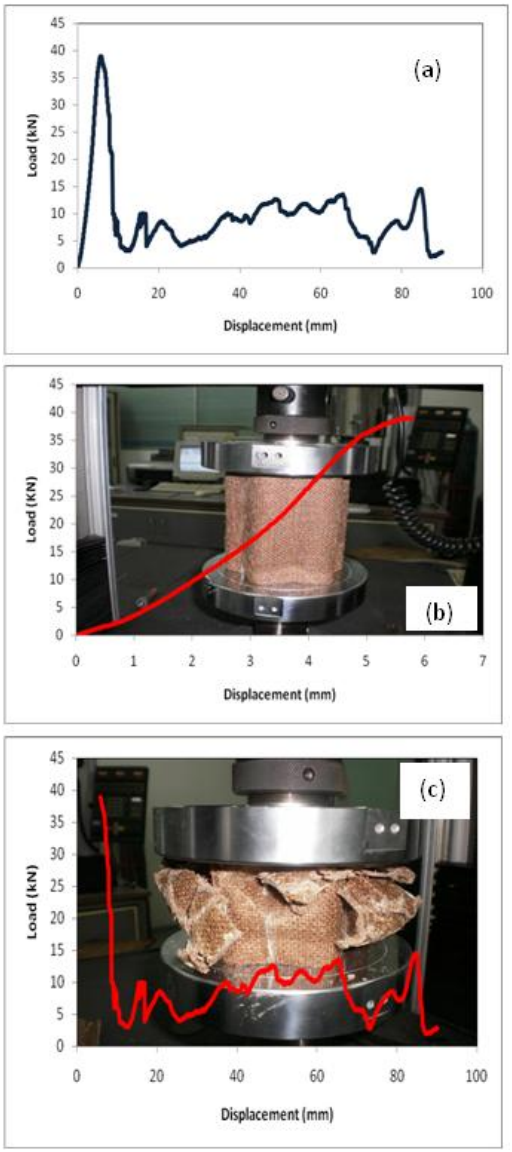

Fig. 13 Load-Displacement Curve of RCJFT

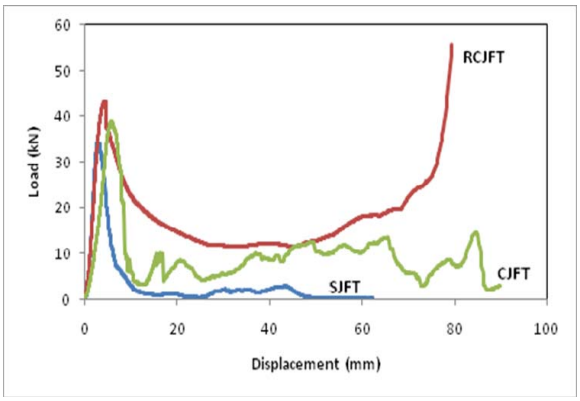

Fig. 14 Load Displacement Curves of Different Geometry

TABLE IV
CRUSHING LOADS OF THE SPECIMENS

ID	F_i (kN)	F_{av} (kN)	F_{max} (kN)	Di (m)	Df (m)	LR
SJFT	34.85	7.08	34.85	0.00282	0.06	1
CJFT	45.35	20.36	45.35	0.00444	0.07	1
RCJFT	38.84	11.34	38.84	0.00577	0.09	1

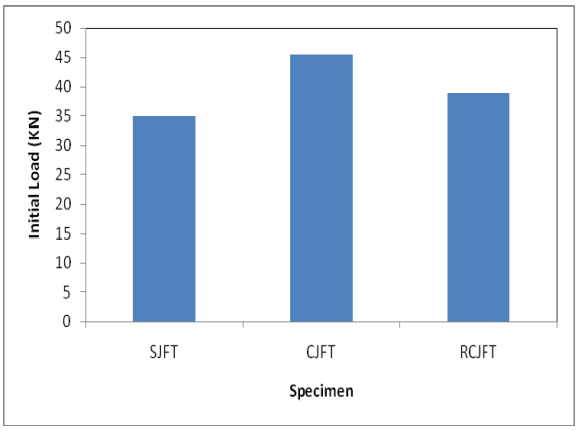

Fig. 15 Initial failure load (Fi) of the specimens

- *Total energy absorbed (EA)*

The total energy absorbed (TEA) is the area under the load–displacement curve. It is a function of the specimen cross-sectional area and the material density. This energy can be obtained by numerical integration of the load displacement curve. Figure 16 shows the values of energy absorption (EA) for the three types of geometry obtained by variable design of jute fabric/epoxy resin. The highest value of 1.43 kJ is obtained by the circular tube (CJFT). The corrugated tube (RCJFT) has higher energy absorption than that of the square tube (SJFT), which has the lowest energy absorption (EA).

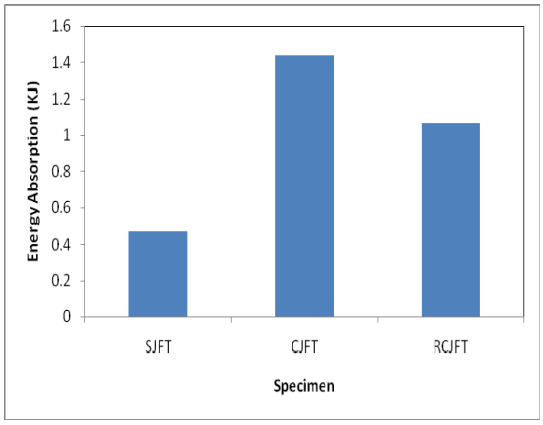

Fig. 16 Total Energy Absorption (TEA) of the specimens

- *Specific energy absorption (SEA)*

Specific energy absorption (SEA) is the energy absorbed per unit mass of material, and the units of SEA are kJ/kg. Figure

17 depict that the circular tube CJFT produced the highest values of specific energy absorption. Therefore, the circular geometry is the best for the appliances designed with the jute fiber/epoxy resin.

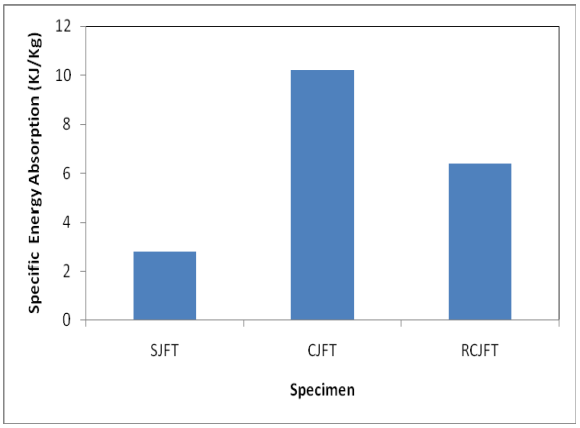

Fig. 17 Specific Energy Absorption (SEA)

- *Volumetric Energy Absorption (VEA)*

Volumetric Energy Absorption (VEA) is the ratio between the energy absorption to the volume of the specimen. The unit is kg/ m^3. Figure 18 presents the variation of volumetric energy absorption VEA with the design of specimen by jute fiber/epoxy resin. The highest value was obtained by the circular tube CJFT which also corresponds to higher energy absorption EA. The corrugated tube RCJFT generated a lower value of VEA, 87.5% and the square tube generated the lowest 25% of VEA obtained in case of CJFT.

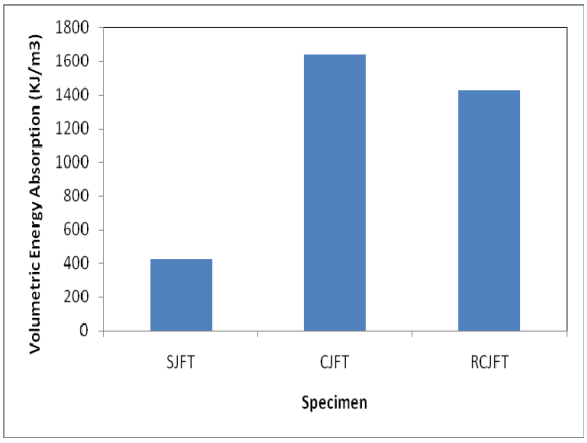

Fig. 18 Volumetric Energy Absorption (VEA)

Crashworthiness parameters of the three specimens are listed in Table 5.

TABLE V
CRASHWORTHINESS PARAMETERS OF THE SPECIMENS

	SQJFT	CJFT	RCJFT
Mass (Kg)	0.169	0.141	0.167
Volume (m3)	0.00111	0.00087	0.00075
EEA(kJ)	0.04913	0.100677	0.112068
PEA(kJ)	0.42182	1.336939	0.955965
EA(kJ)	0.47096	1.437616	1.068034
SEA(kJ/kg)	2.78	10.19	6.39
VEA(kJ/m3)	422.33	1642.27	1425.94

IV. CONCLUSIONS

1. The brittle fracture failure initiates either at the SJFT or at the RCJFT in other word, at structures included corners or corrugated walls.
2. Crashworthiness capability of jute composite significantly depends on the geometry of the specimen. The circular jute composite tubes generated the highest value of Fi, Favg, EA, SEA and VEA and thus the circular geometry is the best among the appliances which deal with the jute fiber/epoxy resin design.
3. The high value of initial load and strain of the jute fiber tubes lead to high energy fracture.

REFERENCES

[1] Sands, J. M., Fink, B. K., McKnight, S. H., Newton, C. H., Gillespie Jr., J.W., Palmese, G. R.. Environmental issues for polymer matrix composites and structural adhesives. *Clean Products and Processes*, 2, 4, 2001, February, pp. 228-235.
[2] [2] Joshi, S.V., Drzal, L.T., Mohanty, A.K., Arora, S. Are natural fiber composite environmentally superior to glass fiber reinforced composites. *Composites: Part A* (35), 2004, pp. 371-376.
[3] [3] Dweib, M.A., Hu, B., O'Donnell, A., Shenton, H.W., Wool, R.P. All natural composite sandwich beams for structural applications. *Composite Structures*, 2004, 63, pp. 147-157.
[4] [4] Williams, George I. and Wool, Richard P. Composites from Natural Fibers and Soy Oil Resins. *Kluwer Academic Publishers*, 2000, pp. 421-432.
[5] [5] Franck, Robert R. *Bast and other plant fibres. Woodhead Publishing in* Textiles. The Textile Institute, 2000, pp. 94-175.
[6] [6] Lamy B, Pomel C, Influence of fiber defects on the stiffness properties of flax fibers-epoxy composite materials, Journal of Materials Science Letters 21, 2002, pp. 1211-1213.
[7] [7] Santulli C, Mechanical and impact properties of untreated jute fabric reinforced polyester laminates compared with different E-glass fibre reinforced laminates, Science and Engineering of Composite Materials 9, 2000, pp. 177-188.
[8] [8] Santulli C, Post-impact damage characterisation in natural fibre reinforced composites using acoustic emission, NDT&E International 33, 2001, pp. 531-536.
[9] [9] Santulli C, Cantwell WJ, Impact damage characterisation on jute/polyester composites, Journal of Materials Science Letters 20, 2001, pp. 477-479.
[10] [10] Abrate S, Impact on composite structures, Cambridge University Press, 1998.